Optimization Model for Charging Infrastructure Planning with Electric Power System Reliability Check

Sreten Davidov, Miloš Pantoš

University of Ljubljana, Faculty of Electrical Engineering, Tržaška 25, SI-1000, Ljubljana, Slovenia
E-mail: sreten.davidov@fe.uni-lj.si, milos.pantos@fe.uni-lj.si

Abstract

This paper presents a significantly improved optimization model for the planning of the charging infrastructure for electric-drive vehicles, where the optimization objective function is the minimization of overall (installation, maintenance, operation) placement costs of charging stations with regards to a charging technology. The constraints involve the electric power system reliability check, ensuring charging reliability and the required quality of service of the charging infrastructure. In ensuring the charging reliability, at least one candidate location must be selected within the driving range of electric vehicles and suitable charging technologies placed to accommodate the disposable charging times of electric vehicle users for the requested quality of service. The proposed optimization model presents an upgrade of an existing optimization formulation since it includes a power system reliability check based on a DC power flow model. To show the general applicability and significance of the model, a test 10×10 grid road network and a standard six-bus test power system are considered. Numeric results illustrate the optimal charging stations placement layout and overall costs placement for different driving ranges and the required quality of service level by including a power system reliability check, to serve both the charging infrastructure investors and electric power system operators.

Keywords

power system reliability check, charging reliability, charging stations, electric-drive vehicles, DC power flow model, quality of service.

1. Introduction

In recent years, electric-drive vehicles (EV) have been gaining importance as an alternative transportation option, mainly stimulated by governmental purchasing premiums due to their positive environmental impact, lower transportation costs and noise, [1]. Existing vehicle manufacturers are planning to end the diesel engine vehicles production and to develop serial production of alternative energy propelled vehicles, [2]. The costs of the battery packs for EVs are failing rapidly, [3], which can make the EV purchase easier. Thus, in the near future there will be more EVs circulating on the roads and loading the power network, which requires proper planning of the charging infrastructure.

In the last decade, researchers from both electrical and transportation communities have published their research on optimal charging infrastructure (CI) location placement. Representative papers are [4]-[7], which mainly include developing a framework and models to capture the charging needs based on the EVs movement and to place the CI optimally at lowest costs regarding the constraints imposed by the road and power networks. In [7], the model has included the driving data of the EV drivers' behavior to present the optimal charging stations layout. Especially higher significance is given to the fact that the electric power system (EPS) reliability check has to confirm the allowed operational limits and power balance in the network as highlighted in [8]. Reference [9] points out that the significant load due to the charging needs of EV users may overload network elements, increase network active power losses and violate the EPS operation. In some cases, the renewables can violate the normal operation of the EPS due to their stochastic behavior and increase the functional uncertainty in the power network. Hence, in [10], it is shown how EVs can help integrate renewables by smart charging strategies with different EV fleets which are limited by their state-of-charge, charging time duration and battery cycles. Since the integration of renewables requires operational flexibility, the V2G (vehicle-to-grid) option in the inclusion of the EV fleet has an effect on smoothing (reducing) the spot market prices, as noted in [11]. The complementary operation of CSs should result in a higher EPS reliability, the security of power supply and standard power quality. CI placement methodology that has considered the power

quality at distribution level is presented in [12], by executing a hybrid optimization algorithm and an area distribution system as case study. However, an inadequate CSs location selection and connection to the power grid can straightforwardly lead to the power supply shortage. EV users' charging needs can overlap with daily load peaks or the EPS load increase during critical network switching conditions. The power shortage may be compensated by increasing generation outputs; however, it will consequently push the EPS to its reliability margins, which will eventually end with an EPS element outage, [13]. Alternatively, an optimal EVs charging scheduling can be employed as solution to flatten the "duck curve", as shown in [14]-[17]. According to [16], there were used pre-timed charging schedules to characterize the potential for carbon dioxide emission reductions across charging characteristics, regional driving, and marginal energy generation trend. Another option different from charging scheduling is to involve a hierarchical framework for a coordinated charging of EVs as shown in [18].

The closes references to the research presented in this paper are [19]-[21], since they elaborate optimization models where the objective function is set on minimizing the overall placement cost of the CI by simultaneously considering both the reliability of the EPS and the road network, which can be proceeded to calculate the lines' outage criticality. The EV driving range and a flow-capturing method are included to find the charging demand needs. In this paper, in heading 2.2, the EPS reliability check is involved in the model by using the LP formulation to set a DC model for the power flows calculation. In conclusion, the models shown in [19]-[21], address the reliability of the EPS; still, they do not offer a model that includes both the charging reliability of the CI and the requested Quality of Service (QoS) by the EV users, as these additional constraints, as latter shown, affect the final CSs selection and placement costs.

The main purpose of this paper is to help network operators to acknowledge about the lines' outage criticality by integrating the EPS reliability check and to show to CI investors the optimal CSs location selection. Therefore, new, more comprehensive model is proposed followed by a ranking procedure. The ultimate goal to come more closely to reality of CSs placement and to provide valuable information for the CI investors and network operators.

Among the recently published papers, [22] presents an optimization model for CS placement in order to minimize the overall cost by satisfying the charging reliability and the QoS expected by EV owners/drivers. These two key performance indicators (KPI) are noted as following: Charging reliability of the CI is a criterion, defined as selecting at least one location within the driving range of EVs, with the purpose to exceed their mobility limitation, [22]. The QoS is defined as a measure that considers the disposable charging time of EV users needed to complete their planned trips, [22].

The following facts served as incentives for the research presented in this paper:

- the implementation of the EPS reliability check into the previously developed model for optimal CSs placement at minimal cost, fully elaborated in [22]. EPS reliability check is another KPI, defined as a criterion to evaluate the operational limits of the elements and keep the power-flow balance in the EPS with the newly placed CSs of different charging technology to satisfy the EVs charging demand. The literature overview above shows that scarce attention has been given to the issue of involving the EPS reliability check alongside the requested QoS and ensuring the CI charging reliability to help network operators to acknowledge the lines outage criticality, where if ranked, further network activities can be planned such as reconstruction, reinforcement etc.;
- the increasing interdependency of CSs operation and the EPS reliability due to the mass adoption of EVs, [23];
- CI planners' and EPS operators' concerns for their coordinated operation and networks expansion resulting in a reliable power supply;
- the required consideration of the EPS elements' operational limits and discrepancy balance in order to provide a reliable power supply;
- the necessity to incorporate an integrated model of the EPS and road network as an essential precondition for future expansion planning;
- the necessity to engage cost-efficient methodologies that can comprise large-scale interdependent EPSs and road networks.

Thus, the main scientific contributions of this paper, and hence improvements with regards to [19]-[21], include:

- A proposal for an improved optimization model for CSs placement based on the model presented in [22]. Additional improvement with regards to that model, is incorporation of EPS reliability check based on the DC power-flow equations in order to ensure that the EPS operates within the operational limits and provides a sufficient supply to the system load and fulfils the EVs charging needs. Up until now, there is no model that incorporates the EPS reliability check while meeting the requirements of the EV users with respect to their requested QoS and driving range.
- Comparison of the reference and improved model regarding the placement costs, selected locations and number

of selected locations for different case scenarios of the driving range and QoS.

The remaining sections of the paper are organized as follows: a detailed explanation of the improved optimization expansion planning procedure for CSs placement considering the EPS reliability check is presented in Section 2, while Section 3 presents the numerical results. Finally, the conclusion drawn from this paper is discussed in Section 4.

2. Optimization Model for Charging Infrastructure Planning with Electric Power System Reliability Check

Figure 1 presents the proposed optimal expansion planning procedure for CSs placement considering the EPS reliability check, which latter serves to rank the lines' outage by their criticality.

Input data includes the models of the EPS and the road network, a set of charging technologies and costs, EV trajectories and the requested QoS level. The road network is presented as discrete set of candidate location points, as shown in Subsection 2.1.1. The formation of sets representing EV drivers' trajectories is explained in detail in Subsection 2.1.2. The traffic flow weights represent the number of EVs passing through a candidate location in the modelled road network. Weight identification is shown in detail in Subsection 2.1.3.

The EV driving range is a key factor for determining the locations of CSs necessary for completing longer trips, as presented in [22]. Therefore, Subsection 2.1.4 elaborates the formation of the charging reliability criterion. Charging technologies and their charging powers are elaborated in Subsection 2.1.5, while Subsection 2.1.6 presents the overall (installation, maintenance, operation) costs for placing a charging technologies type at a candidate location in the road network. A detailed elaboration for the requested QoS of the CI is presented in Subsection 2.1.7. The modelling of the EPS reliability check is described in Subsection 2.1.8.

Following the input data preparation, the proposed optimization model for CSs placement planning with the EPS reliability check is executed. Consequently, the numeric results show the optimal CSs placement plan.

2.1. Input data preparation

The input data preparation is the first step of the optimization procedure for CSs placement that involves the definition of tasks presented in Subsections 2.1.1 - 2.1.8.

2.1.1. Road network discretisation

One of the main characteristics of this paper is a simple representation of candidate locations in the road network. The *i*-th candidate location point or the m_i is an element of the *M* finite set of *I* candidate locations, defined as follows:

$$M = \{m_1,\ m_2,...,\ m_i,...,\ m_I\};\ i = 1,\ 2,...,\ I \tag{1}$$

2.1.2. Mobility behaviour

EV users follow certain spatial and temporal trajectory patterns, based on their daily habits and transportation needs. These trajectories can be stochastically derived and thus by using a trajectory reduction procedure, reduced to a specific number of trajectories to be used in the optimization procedure, as shown [24]. Therefore, for the EV users, their mobility behavior can be represented by driven trajectories at defined time instances to be included in the optimization procedure.

Hence, the individual EV user mobility behavior is noted as follows:

$$\begin{gathered} N_{v,t} = \left\{n_{v,1,t},\ n_{v,2,t},...,\ n_{v,j,t},...,\ n_{v,J_{v,t},t}\right\}; \\ \forall\ v = 1,\ 2,...,\ V;\ \forall\ t = 1,\ 2,...,\ T \end{gathered} \tag{2}$$

where $N_{v,t}$ is the set representing the *v*-th EV trajectory within the modelled road network at the *t*-th time instance, while $n_{v,j,t}$ is the *j*-th element of the finite set of the EV trajectory. The overall number of observed time instances is noted with *T* time instances. $J_{v,t}$ stands for the *v*-th EV and the overall number of elements of the trajectory at the *t*-th time instance, while *V* is the total number of EVs.

2.1.3. Traffic load weights identification

The traffic load weight represents the number of EVs passing through a candidate location in the modelled road network. It can be identified by analyzing the mobility behavior of EV drivers. In the previous sections, the road network and the trajectories of movement of the EVs are defined as sets, which makes it easy to derive the traffic load weight for candidate locations in the road network. To calculate the weights, the following coefficient is defined:

$$W_{i,t} = \begin{cases} 1, \text{ if } m_i \in N_{v,t} \\ 0, \text{ otherwise} \end{cases}; \ \forall\ t = 1,2,...,T; \\ \forall\ v = 1,2,...,V; \ i = 1,2,...,I \tag{3}$$

where the $W_{i,t}$ coefficient takes the value of 1, if the i-th candidate location point is part of the set of trajectory of the v-th EV at the t-th time instance, otherwise it equals 0. The weight of the i-th candidate location point for placing a CS, expressed by w_i, is calculated as the sum of $W_{i,t}$ coefficients in the observed optimization period with the T time instances, noted as:

$$w_i = \sum_{t=1}^{T} W_{i,t}; \ \forall\ i = 1,2,...,I \tag{4}$$

2.1.4. Charging reliability of the charging infrastructure

Since the main disadvantage of EVs in comparison to conventional vehicles is their short range, which, if seen from the CI planners' perspective, can be exceeded by placing CSs at locations that are within the range of EVs and will ensure unlimited mobility. Based on this logic, the general methodology for the charging reliability principle is elaborated in detail in [22], where the charging reliability of the CI is dependent on the EV driving range or R_v. The well-known Euclidean distance, [25], is used as a distance measurement for determining which candidate locations should be placed in the road network. In addition, the Euclidean distance measurement, ξ, is defined as follows:

$$\xi = \sqrt{(m_i - n_{v,j,t})_{dx}^2 + (m_i - n_{v,j,t})_{dy}^2}; \\ m_i \in M; \ n_{v,j,t} \in N_{v,t} \tag{5}$$

where ξ is the Euclidean distance between the i-th candidate location point or m_i and the v-th EV, the j-th trajectory set element at the t-th time instance or $n_{v,j,t}$. The dx and dy values represent the coordinate directions.

The elements that are part of the sets computed in terms of the Euclidean distance between the trajectory set element $n_{v,j,t}$ and the candidate location m_i are noted with $S_{v,j,t}$, which is defined as follows:

$$S_{v,j,t} = \{m_i \in M : \xi \le R_v\}; \\ j = 1,\ 2,...,\ J_{v,t}; \ \forall\ v = 1,\ 2,...,\ V; \\ \forall\ t = 1,\ 2,...,\ T \tag{6}$$

In (6), the elements of the finite set $S_{v,j,t}$ represent all candidate locations in the road network, m_i, which meet the distance criterion $\xi \le R_v$ for the v-th EV at the t-th time instance. To provide a more straightforward notation of candidate locations, the Boolean coefficient, i.e. $a_{i,v,j,t}$, which is equivalent to the set defined in (6), is applied.

$$a_{i,v,j,t} = \begin{cases} 1, \text{ if } \xi \le R_v \\ 0, \text{ otherwise} \end{cases} \tag{7}$$

The $a_{i,v,j,t}$ coefficient in (7) notes whether the distance from the i-th candidate location to the j-th trajectory set element for the v-th EV at the t-th time instance falls within the scope of the defined distance criterion, $\xi \le R_v$. If this criterion is met, the $a_{i,v,j,t}$ coefficient takes the value of 1, otherwise its value equals 0.

With respect to the current development of battery technologies, this paper assumes that the formation of sets in (6) according to a Euclidean distance measurement satisfies the well-known 'distance to empty' criterion, [26]. According to this definition, the complete charging reliability of a CI is achieved when a location is selected within the driving range of the EVs considered in the planning of the CI. The elements of the individual Sv,j,t set would thus represent those candidate locations that fulfil the given distance criterion (i.e. $\xi \le$ Rv). In order to explain the charging reliability clearly, a simple example is presented in Figure 2, which assumes that an EV wishes to go from point A to point B, as shown in Figure 2(a). In the present paper, the notation of the circle center is introduced as a location of the CS, while the radius of the circle represents the driving range of the EV. Figure 2(a) shows that the end point B cannot be reached by starting from point A due to the range limitation of the EV. In order to achieve conceptuality and make the example clearer, it is presumed that the battery of the EV is fully charged at point A. The EV driver would then drive a distance equal to the driving range and run out of charge, i.e. the EV would not complete the intended trip. Figure 2(b) shows a CS, which is placed at the end point B. Yet again, the EV starting from A would not reach B, since it can only drive for a distance equal to the driving range value and would run out of charge before arriving to end point B. In addition, the charging reliability is not ensured in this case, which means that no CS is placed at a location that can

be reached within the driving range. Figure 2(c) demonstrates the principle, which is the basis for ensuring the charging reliability of the CI. Starting from point A, a CS2 is placed within the driving range of the EV, so it can reach point B and thus complete the trip. The centers of overlapping circles represent the location of charging stations.

2.1.5. Charging technologies

The charging technology dictates the charging time, since higher charging powers can provide shorter charging times. Equation (8) notes the charging time of a charging technology for a travelling distance equal to the EV driving range:

$$L_{k,v} = CT_k / R_v; \quad \forall\, v = 1, 2, ..., V;\ \forall\, k = 1, 2, ..., K \tag{8}$$

where CT_k is the charging time using the k-th charging technology to reach a distance equal to the initial EV driving range, i.e. R_v.

The charging power of the k-th charging technology is P_k. This is the plug-in active power if the k-th charging technology is installed at a candidate location. This parameter is factored in the EPS reliability check.

2.1.6. Costs for placing a charging station

The overall (installation, maintenance, operation) costs for placing a CS at a candidate location vary and are predominately dependent on the candidate charging technology to be installed. In this paper, the overall costs for placing the k-th charging technology at the i-th candidate location in the road network are noted with $c_{i,k}$.

2.1.7. Quality of Service of the charging infrastructure

The QoS of the CI is profoundly elaborated in [22]. In this paper, the same definition is used. Therefore, the requested QoS_v for the v-th EV driver is defined as follows:

$$QoS_v = DCT_v / D_v;\ \forall\, v = 1, 2, ..., V \tag{9}$$

where DCT_v stands for the overall disposable charging time of the v-th EV driver necessary to reach the overall travel distance D_v.

2.1.8. DC power flow equations

The EPS model is based on equations for the direct current (DC) power-flow calculations which are convenient for the EPS reliability check and defined with the following equations:

$$\mathbf{A} \cdot \mathbf{PG} - \mathbf{B} \cdot \mathbf{PD} - \mathbf{W} \cdot \mathbf{PL} = \mathbf{0} \tag{10}$$

$$PL_r = \frac{\theta_{m,r} - \theta_{n,r}}{x_r};\ \forall\, r = 1, 2, ..., R \tag{11}$$

$$|PL_r| \le PL_r^{\max};\ \forall\, r = 1, 2, ..., R \tag{12}$$

$$PG_g^{\min} \le PG_g \le PG_g^{\max};\ \forall\, g = 1, 2, ..., G \tag{13}$$

$$\theta_{ref} = 0 \tag{14}$$

Equation (10) notes the power-flow balance in the EPS. **A** is the bus-generation unit incidence matrix, while **PG** represents the matrix of generator unit outputs. **B** stands for the bus-electric load incidence matrix, while **PD** is the matrix of bus electric loads. **W** represents the bus-transmission line incidence matrix, **PL** denotes the matrix of power flows, while **0** is the vector of zeros. R stands for the overall number of lines, while G stands for the overall number of generators in the EPS.

PD is the matrix that comprises the PD_q elements and is defined as follows:

$$PD_q = PD_0 + \sum_{i \in \Gamma_q} \sum_{t \in \Phi} \sum_{k \in \Theta} P_k \cdot x_{i,t,k}; \quad \forall\, q = 1, 2, ..., Q \tag{15}$$

PD_0 stands for the base EPS load connected on the q-th bus. P_k denotes the charging power of the k-th candidate charging technology. Γ_q is the subset of candidate locations connected to the q-th bus, while Φ and Θ are the subsets denoting the time instances over the optimization period of the T time instances and the K candidate charging technologies of the connected candidate locations to the q-th bus, respectively. Q stands for the overall number of

busses in the EPS.

In (11), the r-th line power flow depends on the value of the r-th line reactance, x_r, and the difference of the m-th and n-th connection bus angles for the r-th line, i.e. $\theta_{m,r}$ and $\theta_{n,r}$, respectively. R stands for the overall number of lines in the EPS. The maximum flow value for the r-th line or PL_r^{max} is noted in (12). Equation (13) denotes the maximum limit, PG_g^{max}, and minimum limit, PG_g^{min}, values for the g-th generation unit output or PG_g. The value of the reference bus angle is noted in (14).

2.1.9. Lines outage criticality ranking

Lines are ranked regarding to their outage criticality, IC_r, which is determined as ratio of power flow of r-th line, PL_r, and r-th line maximal thermal capacity, PL_r^{max}. This is normalization to the maximal line capacity, still, the r-th line power flow includes the additional demand required to charge the EVs, as noted in equation (15). Thus, if the ratio is near the r-th line maximal capacity, i.e. high value of the IC_r, are critical, since they operate near their maximal limit and hence have higher line outage possibility. In this context, the network operator oversees where additional investing must be done to face the charging demand due to the EVs.

$$IC_r = \frac{PL_r}{PL_r^{\max}} \;\forall\; r = 1,\; 2,\ldots,\; R \tag{16}$$

In the final step, a priority list is yielded in decreasing order according to the calculated values of the IC_r of r-th line. In comparison to the ratio values, the priority list is acquired as follows:

$$IC_h > IC_e > \ldots > IC_u \tag{17}$$

IC_h represents the h-th individual line ratio value exposing that h-th line is most critical, and needs to be reconstructed, reinforced etc. IC_e is the next e-th line outage criticality ratio value to follow, up until the last u-th line of the power network. The sequences of the outage criticality indices in (17) can differ, which depends on the optimal selection layout and the variety of the input data for the optimization model shown in Subsection 2.1.

2.2. Optimal charging stations placement model considering electric power system reliability check

The objective function presented in (18) minimizes the overall costs for placing CSs by applying the K charging technologies and I points in the road network in an optimization period of the T time instances. The w_i parameter, as shown in (4), denotes the traffic flow through a candidate location and represents the importance of the i-th candidate location point for placing a CS. As already stated in Subsection 2.1.3, the points with higher weight are of higher importance, since a higher traffic flow has a subsequent effect on a higher charging demand. The overall costs for placing the k-th charging technology at the i-th candidate location are noted with $c_{i,k}$.

$$F = \underset{\Omega}{\text{minimize}} \sum_{t=1}^{T} \sum_{i=1}^{I} \sum_{k=1}^{K} \frac{1}{w_i} \cdot c_{i,k} \cdot x_{i,t,k} \tag{18}$$

The $x_{i,t,k}$ is a binary decision variable associated with the k-th charging technology to be placed at the i-th candidate location point at the t-th time instance, while Ω is the overall set of $x_{i,t,k}$ optimization variables.

In addition to the EPS reliability check equations, i.e. equations from (10) to (14), other optimization constraints include:

$$\begin{gathered} \sum_{i=1}^{I} a_{i,v,j,t} \cdot x_{i,t,k} \geq 1;\; j = 1,2,\ldots,J_{v,t}; \\ t = 1,\ldots,T;\; v = 1,2,\ldots,V;\; k = 1,2,\ldots,K \end{gathered} \tag{19}$$

In accordance with the charging reliability principle elaborated in Subsection 2.1.4, a constraint in (19) is introduced to ensure the charging reliability of a CI by using the $a_{i,v,j,t}$ coefficient, as presented in (7).

$$\begin{gathered} \sum_{i=1}^{I} \sum_{k=1}^{K} L_{k,v} \cdot x_{i,t,k} \leq QoS_v; \\ t = 1,\ldots,T;\; v = 1,2,\ldots,V;\; k = 1,2,\ldots,K \end{gathered} \tag{20}$$

The left-hand side of the constraint presented in (20) ensures the placement of the k-th charging technology at the i-th candidate location with a charging time necessary to achieve the EV driver's requested quality of service level or QoS_v.

$$x_{i,t+1,k} = x_{i,t,k};$$
$$t = 1,\ldots,T-1;\ i = 1,2,...,I;\ k = 1,2,...,K \tag{21}$$

The equality constraint presented in (21) is applied to obtain the continuity of the *i*-th candidate location decision variable during the optimization period of the *T* time instances and *K* technologies. If the *k*-th candidate charging technology at the *i*-th candidate location is selected at the *t*-th time instance, the selection decision must be committed to the following *t+1* time instance for the observed time period with the *T* time instances and *K* charging technologies:

$$x_{i,t,k} \in \{0,1\};\ t = 1,2,\ldots,T;$$
$$i = 1,2,...,I;\ k = 1,2,...,K \tag{22}$$

The constraint presented in (22) denotes the binary definition of the *k*-th charging technology installed at the *i*-th candidate location decision variable at the *t*-th time instance, i.e. the binary definition of *I* candidate location points in an optimization period of *T* time instances and *K* charging technologies.

3. Numerical Results

For the purpose of this paper and to expose its' general applicability, a test road network and the standard six-bus EPS test by *Wood* and *Wollenberg*, [27], presented in Figure 3, are used to execute the CSs placement optimization procedure. This case study is made to reveal the concept and the principle used in the presented methodology for optimal locations selection and charging stations placement and, hence, the model with the input data preparation and constraints, can be used to model both road network and power systems of greater size. Explicitly, the discrete and the linear approach are intentionally selected for that purpose, which is in Subsections 2.1.1 - 2.1.9 and 2.2.

The test road network in Figure 3a) consists of $I = 100$ discrete points, which also represent the candidate locations for placing a CS using different charging technology types. All candidate locations hold a notation from 1 to 100 and are equally distributed at a 100 km distance between two consecutive candidate locations. In addition, Figure 3a) also depicts which bus within the EPS candidate locations are connected to. The test EPS in Figure 3b) includes 11 lines, 6 buses and 3 generators. The data for the test EPS is also shown in Figure 3b). EPS quantities are expressed in p.u, i.e. as a function of a defined base unit quantity, which is 100 MVA.

In this paper, the number of candidate charging technologies to be placed at a candidate location is $K = 2$. The first charging technology candidate, i.e. $k = 1$, is a *slow charge technology* with charging time $CT_1 = 240$ minutes, while the second charging technology, i.e. $k = 2$, is the *fast charge technology* with charging time $CT_2 = 20$ minutes. The CSs charging powers or P_k for the slow charge technology are $P_1 = 0.1$ p.u., while for the fast charge $P_2 = 0.5$ p.u, respectively.

Table 1 shows the mobility behavior of EVs, which is noted with the time instances and the trajectory points of movement of the EVs in the road network. This is made to consider and thus optimally select locations for placing CSs at paths that are in accordance with the mobility behavior of EV users. In this case study, three EVs are considered (column 1), which are driven by the EV users in different time instances (column 2). In the considered optimization period, the first EV user has the most diverse time schedule and the third EV user is the most reserved. Therefore, the EVs movement in the road network or their trajectory (column 3), can be noted based on EV users' different habits and transportation needs. The longest and the shortest trajectory noted by its individual trajectory points, stands for the first EV user at 1st and 12th time instance, respectively.

The investment costs for the candidate locations with regard to the *slow charge technology* are varying between 10,000 € and 100,000 €, while for the *fast charge technology* between 100,000 € and 1,000,000 €. The related traffic load weights are calculated by (4) based on the EV trajectories shown in Table 1.

This paper considers two models: a model without the EPS reliability check (reference) and a model with the EPS reliability check (improved). By comparing the two models, the goal is to examine the impact of incorporating the EPS reliability check on the optimal CSs placement layout and the overall CI placement costs. The comparison is made for three different cases of the value of the QoS_v (cases **1**-**3**) and EV driving and EV driving ranges (cases **I-III**), as presented in Table 2.

The first case (case 1) of QoS_v considers that the EV driver has a very short disposable charging time, as presented by the low value of the QoS_v index. A low disposable charging time of the EV driver can be considered as a significant reflection of being in a hurry or having limited time at their disposal, e.g. late for work, meeting, etc.

The second case (case 2) considers a higher disposable charging time, while case 3 considers an example where the EV user has a very long waiting time at their disposal for battery charging and thus reflects that there are no restrictions regarding their on-time arrival.

The R_v is also equal for all EV drivers and the three cases involving a different driving range are explored. To obtain the difference in the comparison models, an optimization execution analysis is conducted for all combinations of individual cases involving the EV driving range and the *QoS* (cases 1.**I**…3.**III**).

Table 2 shows the optimization results for the three different cases and ranges, for the models without and with the EPS reliability check. The Δ_F value corresponds to the difference in the overall CI placement costs. A comparison of results calculated as the Δ_F and presented in Table 2 shows that the CI placement costs for the model with the EPS reliability check (*F'*) are higher in comparison with the model without the EPS reliability check (*F*) due to the new constraints added for the EPS limitations and keeping the power flow balance. The highest difference in the value of placement costs can be observed in the case involving the shortest driving range and low values of the *QoS*, since more CSs with faster charging times need to be placed.

The models' comparison is further made for the different values of the EV driving range by constantly increasing the value of the $QoS_{v,}$ as shown in Figure 4. The initial value of the *QoS* is equal for all EV drivers and starts at 10 min/100 km, after which it is constantly increasing with step 5 min/100 km.

As shown by the comparison curves in Figure 4, the incorporation of the EPS reliability check contributes to increasing the overall CI placement costs for all observed cases. Table 3 acknowledges the difference in the optimal CSs placement location selection for the models without/with the EPS reliability check, respectively. Table 3, column 1, lists the case numbers elaborated in Table 2 with respect to the different values of the QoS and driving range. Case numbers I, II and III note the different values taken for the driving range, 200 km, 400 km and 500 km, respectively. For the case numbers 1, 2 and 3 the values of the QoS are increasing respectively, to note the higher value of the disposable charging times of EV users for their planned trips. Table 3, column 3 (row-wise), notes the selected locations and column 4 (row-wise) the overall number of selected locations, for the individual case number and used model shown in columns 1 and 2. Columns 3 and 4 can serve to expose or detect, how the additional EPS reliability check constraints impact the change in the optimal CSs location selection and overall number of CSs for the studied case. We provide also a graphical example showing the changed and unchanged optimal CSs location selection for the two models in case 1.**III** is presented in Figure 5.

Regarding Figure 5, the optimal locations which are selected in the optimal solution by applying the model without the EPS reliability check and are not selected in the optimal solution by applying the model with the EPS reliability check are considered as changed. Otherwise, an optimal location is considered unchanged, if it is selected in both optimal location selection solutions. In Figure 5, optimal locations no. 14, 16, 42, 92 and 96 remain unchanged, while others, such as number 6, 8, 20, 22, 33, 34, 38, 40, 58, 64, 70, 74, 75 and 78, change.

Table 4 gives a comparison of the lines power flows in the base (column 2) and newly derived states of the EPS (columns 3 - 11) due to the integration of the CSs. Column 1 notes the *r*-th line, column 12 notes the maximum capacity of *r*-th line and column 13, the mean value of the lines' power flow. Lines are ranked regarding to their outage criticality, IC_r, column 14, as shown in equation (16) and (17). To expose which lines are most critical with regards to all the optimization cases, IC_r is determined as ratio of their mean power flow value for all cases and their maximal capacity. Therefore, lines having the highest IC_r are critical, since they operate near their maximal limit and hence have higher line outage possibility. Results show (column 14), that lines 1, 8, 3, 6, 2, 7, 5 and 9 are critical, since on average they operate near the maximal capacity, lines 10, 4 and 11 are not critical.

Figure 6 shows an example of the *F'* vs. PL_r^{max} dependency, for the case of equal increase of the initial lines capacity. At 0 p.u., the lines' maximum capacity is equal to their initial and at 1 p.u., their capacity is doubled. For the input data of the case 1.I, *F'*, starts at 59,679,500 € and decreases as the lines capacities increase. This is due to the fact of relaxing the new constrains of the EPS reliability check regarding the power flow balance and operational limitations of the EPS elements to satisfy the objective function on minimizing the CI placement costs. The constant part of the curve of *F'*, means that, even though the capacity of the lines is increased, the optimization model perceives the criterion on EPS reliability check as shown in Subsection 2.1.4.

4. Conclusions

This paper proposes a optimization model for charging infrastructure planning by involving an electric power system reliability check based on the DC power flow. The constraints include also the charging reliability principle to exceed the mobility range limitation of the electric-drive vehicles and to accommodate the required quality of service by the users. The charging reliability principle is defined as a selection of at least one candidate location within the driving range of an electric vehicle and is included to enforce unlimited mobility for the electric-drive vehicles. The quality of service of the charging infrastructure is considering as the disposable charging time required for electric

vehicle users to reach the overall travel distance. Placing faster-charging technology types costs more, however the charging time is shorter. The effectiveness of the proposed formulation is demonstrated by a case study involving a test road network and a test six-bus electric power system for different driving ranges and required quality of service levels. Two optimization models are compared in each of the cases in order to indicate the significance of the electric power system reliability check which considers the network elements' limitation and the generation-demand balance in the power network. Numeric results show which locations remain unchanged and which change due to additional constraints incorporated in the calculations. The model with the electric power system reliability check shows a different selection solution of optimal locations and higher overall placement costs in comparison with the model without the electric power system reliability check, due to the additional constraints. Further comparisons are made by constantly increasing the required quality of service and applying different values of the driving range. Still, the overall placement costs for the model with the incorporated reliability check remain higher. An outage criticality ranking list is yield, which is valuable for the network operators to acknowledge where to reinforce or reconstruct the power network to face the increasing adoption of electric-drive vehicles in the long therm. This paper represents a solid basis for future work that will consider the employment of linearized approaches for running the electric power system reliability check based on the AC power flow calculation.

5. References

[1] Carlsson, F., & Johansson-Stenman, O. (2003). Costs and benefits of electric vehicles. *Journal of Transport Economics and Policy (JTEP)*, *37*(1), 1-28.

[2] Bozbas, K. (2008). Biodiesel as an alternative motor fuel: production and policies in the European Union. *Renewable and Sustainable Energy Reviews*, *12*(2), 542-552.

[3] Nykvist, B., & Nilsson, M. (2015). Rapidly falling costs of battery packs for electric vehicles. *nature climate change*, *5*(4), 329.

[4] He, F., Wu, D., Yin, Y., & Guan, Y. (2013). Optimal deployment of public charging stations for plug-in hybrid electric vehicles. *Transportation Research Part B: Methodological*, *47*, 87-101.

[5] Sadeghi-Barzani, P., Rajabi-Ghahnavieh, A., & Kazemi-Karegar, H. (2014). Optimal fast charging station placing and sizing. *Applied Energy*, *125*, 289-299.

[6] Dong, X., Mu, Y., Jia, H., Wu, J., & Yu, X. (2016). Planning of fast EV charging stations on a round freeway. *IEEE Transactions on Sustainable Energy*, *7*(4), 1452-1461.

[7] Ye Tao, Miaohua Huang, LanYang: "Data-driven optimized layout of battery electric vehicle charging infrastructure", Energy, Vol. 150, pp. 735 - 744, 2018.

[8] Dharmakeerthi. C. H., Nadarajah Mithulananthan, & T. K. Saha. "Modelling and planning of EV fast charging station in power grid." *Power and Energy Society General Meeting. 2012 IEEE*. IEEE. 2012.

[9] Dharmakeerthi. C. H., N. Mithulananthan, & T. K. Saha. "Planning of electric vehicle charging infrastructure." *Power and Energy Society General Meeting (PES). 2013 IEEE*. IEEE. 2013.

[10] Katrin Seddig, Patrick Jochem, Wolf Fichtner: "Integrating renewable energy sources by electric vehicle fleets under uncertainty", Energy, Vol. 141, pp. 2145 - 2153, 2018.

[11] Philipp Hanemann, ThomasBruckner: "Effects of electric vehicles on the spot market price", Energy, Vol. 162, pp. 255 - 266, 2018.

[12] Abhishek Awasthi, Karthikeyan Venkitusamy, Sanjeevikumar Padmanaban, Rajasekar Selvamuthukumaran, Frede Blaabjerg, Asheesh K.Singh: "Optimal planning of electric vehicle charging station at the distribution system using hybrid optimization algorithm", Energy, Vol. 133, pp. 70 - 78, 2017.

[13] Božič, D., & Pantoš, M. (2015). Impact of electric-drive vehicles on power system reliability. *Energy*, *83*, 511-520.

[14] Le Floch, C., Belletti, F., Saxena, S., Bayen, A. M., & Moura, S. (2015, December). Distributed optimal charging of electric vehicles for demand response and load shaping. In *Decision and Control (CDC), 2015 IEEE 54th Annual Conference on* (pp. 6570-6576). IEEE.

[15] Erol-Kantarci. Melike, Jahangir H. Sarker, & Hussein T. Mouftah. "Quality of service in plug-in electric vehicle charging infrastructure." *Electric Vehicle Conference (IEVC). 2012 IEEE International*. IEEE. 2012.

[16] Christopher G. Hoehne, Mikhail V. Chester: "Optimizing plug-in electric vehicle and vehicle-to-grid charge scheduling to minimize carbon emissions", Energy, Vol. 115, Part 1, pp. 646 - 657, 2016.

[17] Chynoweth. Joshua. et al. "Smart electric vehicle charging infrastructure overview." *Innovative Smart Grid Technologies Conference (ISGT). 2014 IEEE PES*. IEEE. 2014.

[18] Xu. Zhiwei. et al. "A hierarchical framework for coordinated charging of plug-in electric vehicles in China." *IEEE Transactions on Smart Grid* 7.1 (2016): 428-438.

[19] Yao, W., Zhao, J., Wen, F., Dong, Z., Xue, Y., Xu, Y., & Meng, K. (2014). A multi-objective collaborative planning strategy for integrated power distribution and electric vehicle charging systems. *IEEE Transactions on Power Systems*, *29*(4), 1811-1821.

[20] Zhang, H., Moura, S., Hu, Z., & Song, Y. (2016). PEV Fast-Charging Station Siting and Sizing on Coupled Transportation and Power Networks. *IEEE Transactions on Smart Grid*.

[21] Zhang, H., Moura, S. J., Hu, Z., Qi, W., & Song, Y. (2017). A Second Order Cone Programming Model for Planning PEV Fast-Charging Stations. *IEEE Transactions on Power Systems*.

[22] Davidov, S., & Pantoš, M. (2017). Planning of electric vehicle infrastructure based on charging reliability and quality of service. *Energy*, *118*, 1156-1167.

[23] Becker, T. A., Sidhu, I., & Tenderich, B. (2009). Electric vehicles in the United States: a new model with forecasts to 2030. *Center for Entrepreneurship and Technology, University of California, Berkeley*, *24*.

[24] Davidov, S., & Pantoš, M. (2017). Stochastic expansion planning of the electric-drive vehicle charging infrastructure. *Energy*, *141*, 189-201.

[25] Danielsson P-E. Euclidean distance mapping. Comput Graph image Process 1980; 14:227-48.

[26] Rodgers, L., Wilhelm, E., & Frey, D. (2013, August). Conventional and novel methods for estimating an electric vehicle's "distance to empty". In *Proc. of the ASME 2013 International Conference on Advanced Vehicle Technologies*.

[27] Wood. Allen J., & Bruce F. Wollenberg. *Power generation operation and control*. John Wiley & Sons. 2012.

Figure Captions

Table Captions

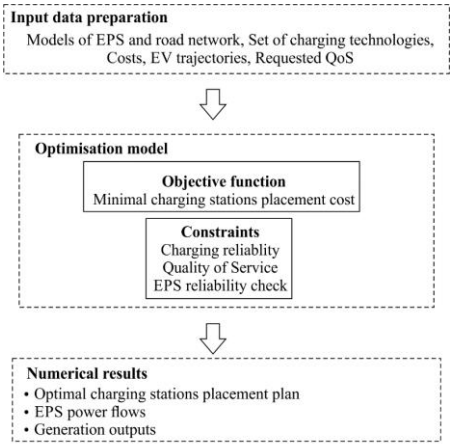

Figure 1 Flow-chart presenting the optimal CSs placement planning procedure with the EPS reliability check

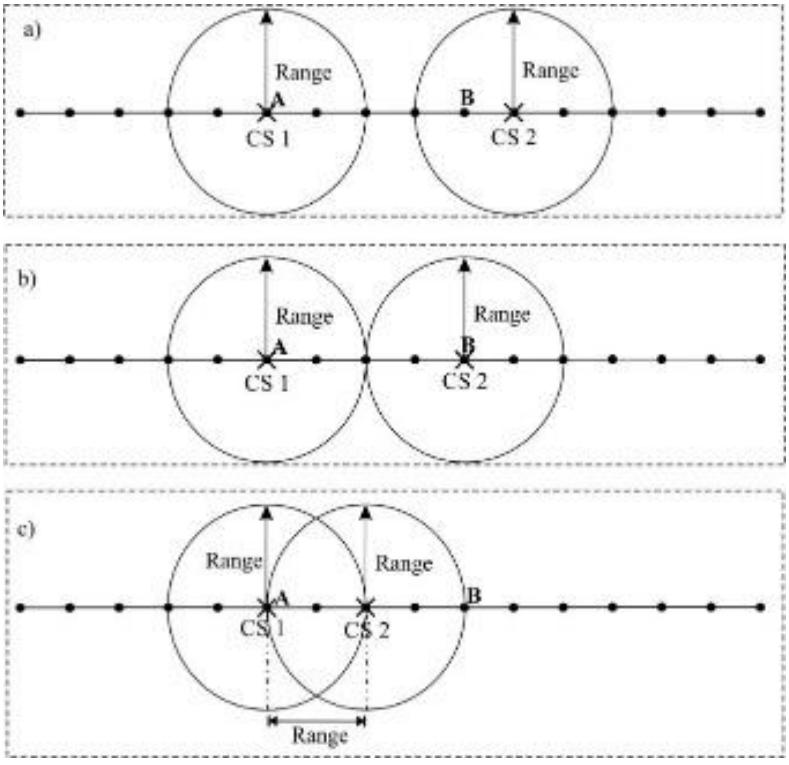

Figure 2 Charging reliability criterion

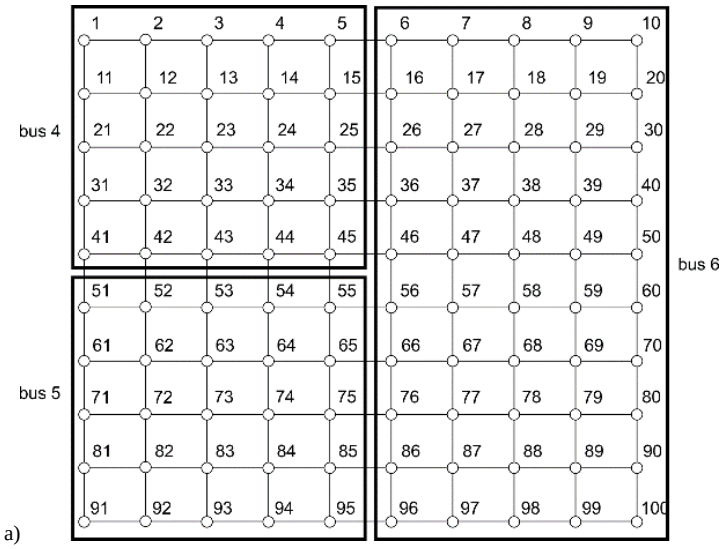

a)

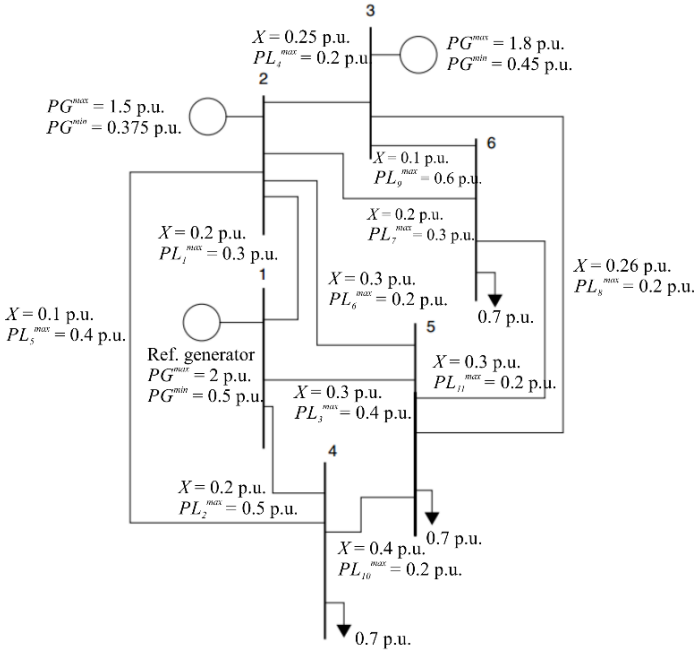

b)

Figure 3 Test road network and bus connections of candidate locations; b) Test EPS with data, [27]

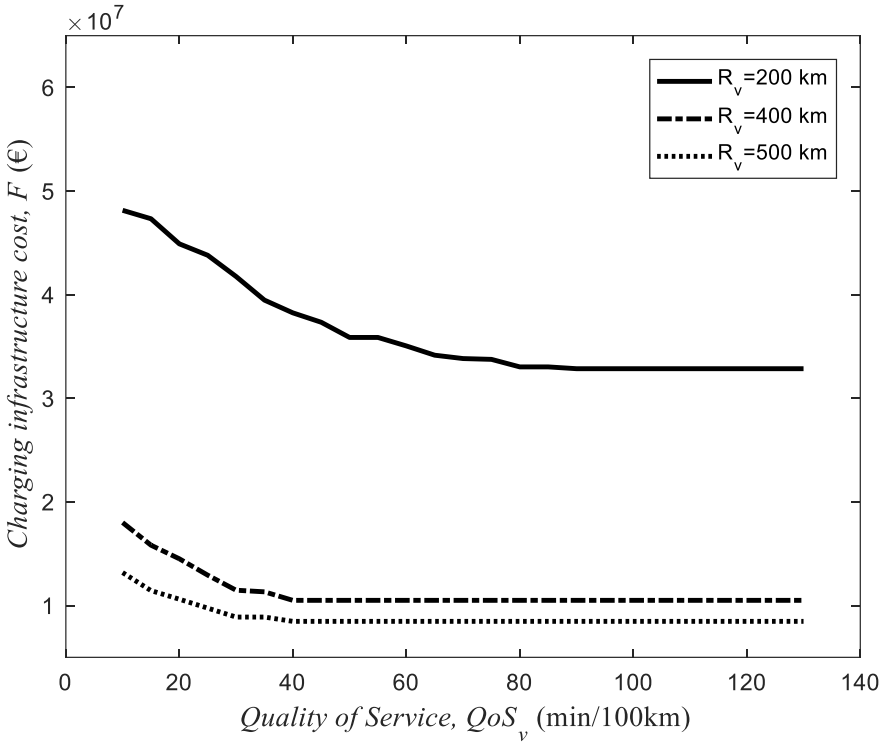

a)

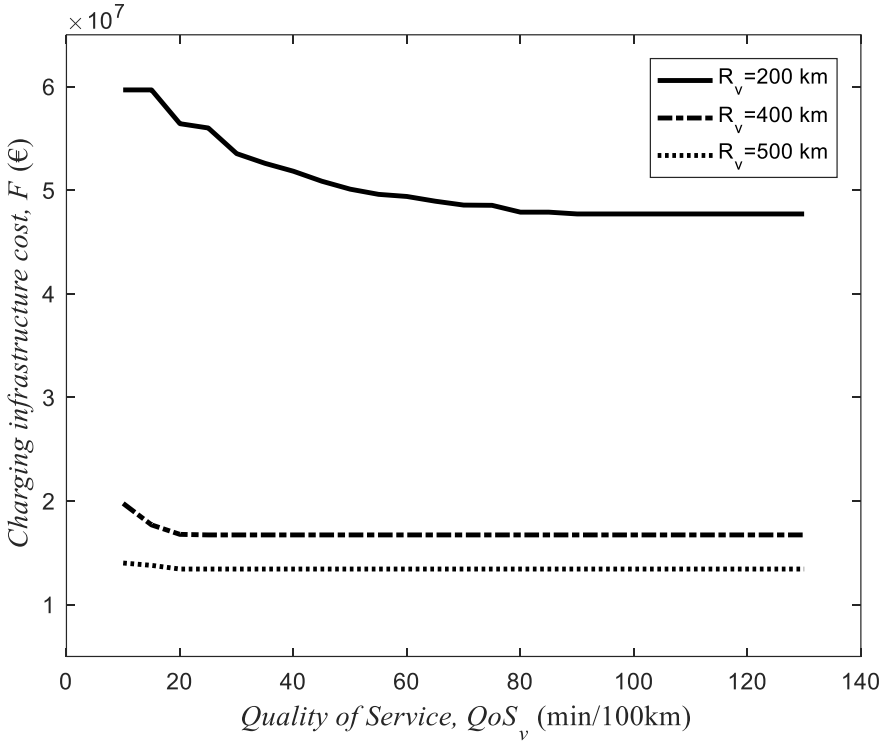

b)

Figure 4 Required QoS_v vs placement costs for different EV ranges: a) without the EPS reliability check b) with the EPS reliability check

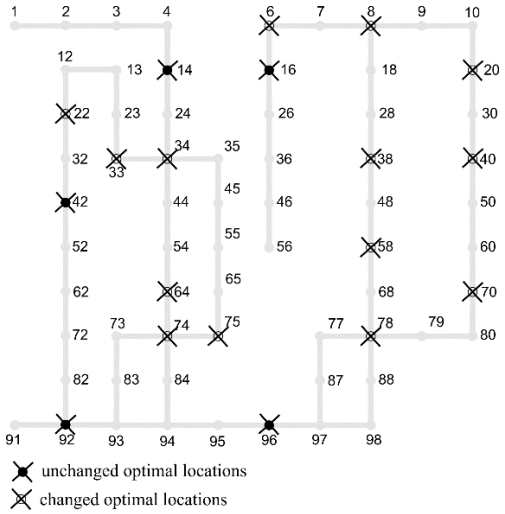

Figure 5 Changed and unchanged optimal locations for the models without/with the EPS reliability check for case 1.**III**.

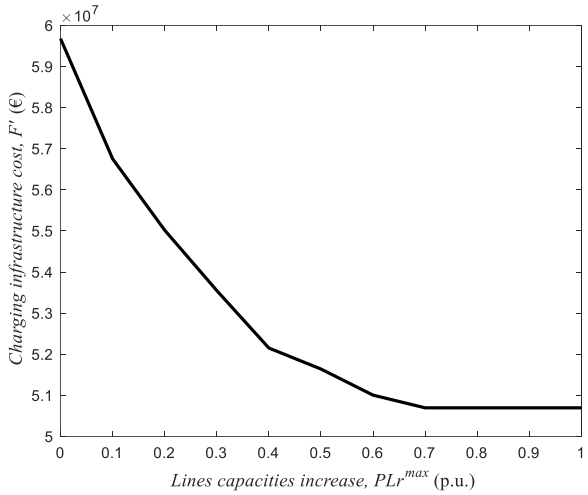

Figure 6 Dependency between the increased initial lines capacity and the charging infrastructure placement cost, *F'*

Table 1 EV trajectories at specific time instances to note EV's mobility behavior

EV	*Time instance*	*Trajectory*
1	t = 1	1 2 3 4 14 24 34 44 54 64 74 84 94 95
	t = 8	95 96 97 87 77
	t = 12	77 78 79 80
	t = 16	80 70 60 50 40 30 20 10 9 8 7 6
	t = 22	6 16 26 36 46 56
2	t = 1	22 32 42 52 62 72 82 92 93 83 73
	t = 15	73 74 75 65 55
	t = 21	55 45 35 34 33 23 13 12 22
3	t = 8	8 18 28 38 48 58 68 78 88 98
	t = 17	98 97 96 95 94 93 92 91

Table 2 Comparison of CI costs as a function of the QoS_v and R_v for the models without/with the EPS reliability check (F and F'), respectively

		I			**II**			**III**		
Case No.	*EV driver*	QoS_v (min/100 km)	R_v (km)	(€)	QoS_v (min/100 km)	R_v (km)	(€)	QoS_v (min/100 km)	R_v (km)	(€)
1	1	10	200	F: 48,403,000 F': 59,679,500 Δ_F: 11,276,500	9	400	F: 18,157,000 F': 20,889,500 Δ_F: 2,732,500	6	500	F: 13,328,000 F': 16,409,000 Δ_F: 3,081,000
	2	11			5			4		
	3	12			4			5		
2	1	42		F: 38,140,500 F': 52,077,500 Δ_F: 13,937,000	35		F: 11,295,500 F': 16,730,500 Δ_F: 5,435,000	25		F: 9,349,500 F': 13,438,500 Δ_F: 4,089,000
	2	45			38			33		
	3	34			26			24		
3	1	130		F: 32,856,000 F': 47,709,000 Δ_F:14,853,000	70		F: 10,500,000 F': 16,730,500 Δ_F: 6,230,500	51		F: 8,472,000 F': 13,438,500 Δ_F: 4,966,500
	2	121			60			83		
	3	117			50			65		

Table 3 Number of CS and selected locations as a function of the QoS_v and R_v

Case No.	*Model*	*Selected locations*	*No. of selected locations*
1.**I**	Ref.	2 3 6 8 10 13 14 18 22 26 30 33 34 38 42 45 46 50 52 54 55 58 70 72 74 75 78 80 83 87 92 94 96 98	34
	Imp.	2 3 6 7 9 13 14 18 20 22 26 33 34 38 40 42 45 46 50 52 54 55 58 70 72 74 75 78 80 83 87 92 94 96 98	35
2.**I**	Ref.	1 3 6 8 10 12 14 18 22 23 26 30 34 38 42 45 46 50 52 54 55 58 70 72 74 75 78 80 83 87 92 94 96 98	34
	Imp.	2 3 6 8 10 13 14 18 22 26 30 33 34 38 42 45 46 50 52 54 55 58 70 72 74 75 78 80 83 87 92 94 96 98	34
3.**I**	Ref.	1 3 6 8 10 12 14 18 22 23 26 30 34 38 42 45 46 50 52 54 55 58 70 72 74 75 78 80 83 87 92 94 96 98	34
	Imp.	2 3 6 8 10 13 14 18 22 26 30 33 34 38 42 45 46 50 52 54 55 58 70 72 74 75 78 80 83 87 92 94 96 98	34
1.**II**	Ref.	3 8 12 20 26 34 38 50 52 74 78 92 96	13
	Imp.	3 6 10 22 26 33 34 38 50 52 74 78 92 96	14
2.**II**	Ref.	3 8 12 26 30 34 38 42 70 74 78 82 93 96	14
	Imp.	3 8 22 26 30 33 34 38 52 70 74 78 92 96	14
3.**II**	Ref.	3 8 12 26 30 34 38 42 70 74 78 82 93 97	14
	Imp.	3 8 22 26 30 33 34 38 52 70 74 78 92 96	14
1.**III**	Ref.	8 14 16 22 34 40 42 58 74 92 96	11
	Imp.	6 14 16 20 33 38 42 64 70 75 78 92 96	13
2.**III**	Ref.	3 8 16 22 34 40 42 58 74 92 96	11
	Imp.	8 14 16 33 38 40 42 64 75 78 92 96	12
3.**III**	Ref.	3 8 16 22 34 38 40 42 74 78 92 97	12
	Imp.	8 14 16 33 38 40 42 64 75 78 92 96	12

Table 4 Comparison of lines power flows and descending ranking of lines according to their outage criticality

r-th line	BASE CASE	CASE 1.**I**	CASE 2.**I**	CASE 3.**I**	CASE 1.**II**	CASE 2.**II**	CASE 3.**II**	CASE 1.**III**	CASE 2.**III**	CASE 3.**III**			
	PL_r (p.u.)	PL_r (p.u.)	PL_r (p.u.)	PL_r (p.u.)	PL_r (p.u.)	PL_r (p.u.)	PL_r (p.u.)	PL_r (p.u.)	PL_r (p.u.)	PL_r (p.u.)	PLr^{max} (p.u.)	PLr^{mean} (p.u.)	IC_r (p.u.)
1	0.30	0.30	0.30	0.30	0.30	0.30	0.30	0.30	0.30	0.30	0,3	0,300	1
8	0.13	0.20	0.20	0.18	0.20	0.20	0.18	0.20	0.18	0.20	0,2	0,194	0,9700
3	0.37	0.38	0.38	0.39	0.38	0.38	0.39	0.38	0.39	0.38	0,4	0,385	0,9625
6	0.17	0.18	0.18	0.19	0.18	0.18	0.19	0.18	0.19	0.18	0,2	0,185	0,9250
2	0.45	0.48	0.48	0.48	0.48	0.48	0.48	0.48	0.48	0.48	0,5	0,482	0,9640
7	0.29	0.27	0.27	0.30	0.27	0.27	0.30	0.27	0.30	0.27	0,3	0,282	0,9400
5	0.30	0.36	0.36	0.37	0.36	0.36	0.37	0.36	0.37	0.36	0,4	0,367	0,9175
9	0.39	0.53	0.53	0.49	0.53	0.53	0.49	0.53	0.49	0.53	0,6	0,525	0,8750
10	0.05	0.04	0.04	0.05	0.04	0.04	0.05	0.04	0.05	0.04	0,2	0,059	0,2950
4	0.07	0.01	0.01	0.04	0.01	0.01	0.04	0.01	0.04	0.01	0,2	0,038	0,1900
11	0.02	0.00	0.00	0.01	0.00	0.00	0.01	0.00	0.01	0.00	0,2	0,023	0,1150